

MODELLING WATER SPRAY – FROM LABORATORY SCALE TO FIRE SAFETY APPLICATION

*Elizabeth Blanchard¹, Pascal Boulet, Pierre Carlotti,
Anthony Collin, Alexandre Jenft, Sullivan Lechêne
CSTB, LEMTA Nancy Université, CNPP*

ABSTRACT

The work described here is a part of a research campaign aiming at improving the understanding of the interactions between water mist spraying and tunnel fire. Several results obtained by present authors during the last five years are reported at various scales. It relies on an extensive use of numerical simulations using the CFD code Fire Dynamics Simulator (FDS, NIST). First, the computational tool is verified and validated on the basis of comparisons with other computational codes and experimentations of increasing complexity: from the laboratory scale for assessing one particular part of the water spray model up to the tunnel scale. For the last case, the code validation makes use of the results of a reduced scale (1/3rd) tunnel fire test campaign conducted between 2005 and 2008. Once the validation is achieved, the computational tool is used intensively in order to improve the understanding of the interaction phenomena between water mist, tunnel longitudinal ventilation and fire. In particular, the water mist influence on the tunnel air flow is studied, the water mist heat contribution is quantified and the heat transferred to the droplets is identified.

INTRODUCTION

The use of water for fire suppression and extinguishment is widespread because water is inexpensive, easy to use and is not hazardous for people and the environment. Today, there exist many ways to produce water droplets intended to be thrown over a fire, the most popular being sprinkler system. The different techniques involved to produce droplets induce a wide range of droplet sizes (from several micrometers to one millimeter or more). We focus here on systems producing the smallest droplets, also called ‘water mist’ systems. Water mist is commonly defined quantitatively by putting an upper limit on the size of droplets (NFPA 750). The use of water mist has grown at a very high rate, starting with the need to find an alternative to the banned halogen-based fire suppressing agents. The generation of fine water droplets offers a number of potential advantages over conventional sprinkler systems. The main difference comes from the fact that breaking water into a cloud of very small droplets greatly increases the surface area available for exchanging heat between water and surrounding gases (Grant 2000, Dubay 1999).

Water Mist Interaction with Fire Environment

There are three major mechanisms related to the presence of small water droplets in the vicinity of a fire. Firstly, a significant amount of heat is transferred from the gases to the water droplets to increase their temperature up to the boiling point, then to evaporate them. This ‘heat sink’ results in a strong air temperature decrease. This cooling also helps reducing the intensity of combustion reactions. Secondly, the phase change from liquid to vapour

¹ *Elizabeth.Blanchard@CSTB.fr*

induces a high volumetric expansion rate consisting of water vapour gas. This phenomenon prevents the mixing between fresh air and combustible vapour, acting like an inerting gas, thus reducing once again the intensity of combustion reactions. Thirdly, if they are small enough, water droplets strongly interact with thermal radiation emitted by fire, tunnel surfaces and surrounding hot gases by absorption and scattering effects (Modest 2003). Water mist then acts as a radiative shield between the flames and the exposed objects (Collin 2010). In addition to these mechanisms, when water droplets strike a solid surface, they may absorb heat, inducing a supplementary heat sink.

Each mechanism importance depends on the fire environment (fire heat release, ventilation, etc.) and on the water mist characteristics (droplet size, spray pattern, etc.). For instance, very small droplets have low initial momentum, so that they are rapidly decelerated after leaving the nozzle. Their residence time in the air is also longer promoting radiative attenuation and gas cooling but their ability to penetrate the flame zone is reduced (Husted 2007), making it difficult to steer them toward a given target. For larger droplet spray, a more important fraction of the injected water falls to the ground or drips over the walls, promoting their cooling and also fire propagation. However, their inertia makes spray penetration in obstructed fire vicinity difficult.

The Use of Water Mist in Tunnels

Fire is a significant threat to safety in tunnels and constitutes an important risk of operating losses. The potential heat release rates of tunnel fires are very high (Ingason 2005). Consequently, the resulting fire conditions can be so severe that manual fire fighting operations is impossible. Recent major fires in the last decades stress the need for a better care to fire safety management in underground facilities (Bergqvist 2005). Besides, requirements for road tunnels have been significantly modified after these tunnel fires. In the particular French case, hazard is estimated for designing the fire safety management based on the ventilation system. This strategy allows to ensure a sufficient safety level in most cases.

Water mist could appear as a promising technique for particular cases such as tunnels involving frequent traffic jam (for instance the Mona Lisa tunnel in Austria where a traffic light is installed at one extremity). Moreover, water mist system installation could allow to get the same fire safety level while reducing the entire safety concept. Water mist could get a breakthrough in egress conditions, fire-fighting operation conditions and fire suppression. For instance, water mist system could directly operate to limit the fire propagation, even to extinguish the fire. In particular, the radiation reduction offered by water mist could be useful to prevent fire extension to other trapped vehicles. However, mitigation system likely interacts with other safety systems and especially the tunnel ventilation.

Thus, a relevant operating of such systems requires a good understanding of interaction between underlying phenomena that occur during a suppressed (tunnel) fire. In that context, all scale tests play an essential part. Laboratory scale tests allow focusing on relatively fundamental phenomena, using simplified test configurations (see for instance refs. (Kincaid 1989, Yoshida 2011)). They also provide interesting data bases for validating computational sub-models. The use of a reduced-scale experimental tunnel has several assets, among them the ability to better characterize the flows and the thermal environment induced by fire, while maintaining reasonable costs. However, there are still some difficulties in properly scaling the thermal radiation attenuation by the sprays and the water droplet size (Heskestad 2002). Large-scale tests are very useful by involving real fire load and fluid flow. However, it could be difficult, and even impossible, to draw general conclusion concerning the influence and the

efficiency of such system. Moreover, such real-scale tests are very expensive because a large number of sensors is required to get a detailed measurement of velocity and temperature fields.

Due to the complexity of the phenomena, the use of computational codes could be essential for improving a posteriori the understanding of the interaction phenomena between water mist, tunnel ventilation and fire. It could even a priori help defining test procedure and it could limit the number of tests by assessing the expected phenomena and their orders of magnitude.

Our work aims at evaluating CFD code contribution in assessing mitigation systems for a real tunnel. It makes use of the Fire Dynamics Simulator (FDS, developed by NIST, USA (see both (McGrattan 2010))). The approach consists in verifying and validating it from laboratory scale up to reduced tunnel scale. Then, the FDS code is used intensively to improve the understanding of the situation. This document is partly extracted from Ref. (Blanchard 2011).

FDS CODE

The FDS code is a 3-D CFD model designed to simulate low-speed, thermally-driven flows. This computational tool is widely used in the fire community, generally to evaluate fire consequences in buildings. FDS has also been used to simulate tunnel fires, especially by McGrattan and Hamins (McGrattan 2001), Cochard (Cochard 2003) and Mawhinney (see (Mawhinney 2011) in particular). The ability of current version of FDS to reconstruct the fire environment from a test performed within the one third test tunnel used here (with a longitudinal velocity too low to prevent back-layering effect and without water mist application) has been presented in details in (Blanchard 2011b). This paper shows that agreement between FDS predictions and temperature measurements is pretty good at different distances from the fire. Air flows are also well reproduced in the simulation, the difference with measurement staying within the overlapping uncertainty limits.

Concerning spray modelling, FDS uses an Eulerian-Lagrangian approach to simulate the turbulent transport of evaporating droplets. This means that trajectories of water droplets are individually tracked. In order to reduce the computational cost, only a limited number of droplets is tracked. Each droplet in the calculation is assumed to represent many others of similar size and trajectory. The droplets tracked have to constitute a representative sample of the entire spray. The spray characteristics are defined at the injection point by several parameters such as fluid thermal properties, droplet size distribution and injection features (spray pattern, volumetric flow rate, etc.). In particular, the droplet size distribution is represented by a probability function that describes the fraction of the water volume transported by droplets whose dimension is less than a given diameter. In FDS, the default probability function is a combination of log-normal and Rosin-Rammler distribution. Droplets trajectories are calculated by solving the momentum conservation. Heat transfer between the droplets and the surrounding gas is computed using correlations preserving the equilibrium with gaseous phase inside each grid cell. When a particle strikes an obstacle, it sticks it (new speed and direction are reassigned) until evaporation.

LABORATORY SCALE

Laboratory scale allows us to focus on a fundamental phenomenon for assessing independently two particular sub-models of the water spray simulation:

- the model yielding radiative transfer through water mist
- the model yielding heat transfer between gaseous phase and water droplets

Radiative transfer (Lechêne 2010)

This problem is related to radiative shielding using a water curtain, rather than being strictly devoted to fire extinction. Two configurations are studied (see Figure 1). Water mist is sprayed by seven nozzles either in the upward direction or in the downward one. Water mist is sprayed between a heat source (an extended blackbody surface 30 cm×35 cm at 773 K) and a target (IR spectrometer matrix by Bruker used as the detector). The measurement involves one acquisition with the spectrometer when the spray is on, then a second with the spray off. The ratio gives a characteristic transmissivity through the spray (or the attenuation by the spray if the complementary part is considered).

Water mist nozzles are located on the same feed pipe and the space between neighbouring nozzles is equal to 10 cm. They produce flat conic sprays, with the larger angles of the cone close to 40 and 110° respectively. Under an operating pressure of 4 bars, flow rate at each nozzle is around 0.32 l.min⁻¹, flow rate number being 8.5.10⁻⁹ m³.s⁻¹.Pa^{1/2}. Mean droplet size in terms of Sauter diameter is 100 μm, 20 cm below the injection point.

The blackbody and the target are translated vertically to measure radiation attenuation through the mist at several heights. On Figure 1, they are located 40 cm high from the nozzle pipe height.

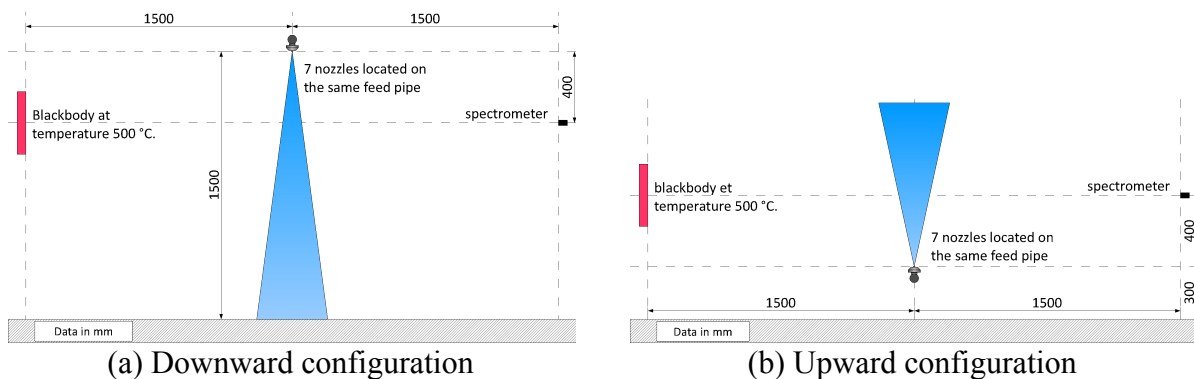


Figure 1: Test configurations for radiative model validation when blackbody and spectrometer are 40 cm high from the nozzle pipe height.

In the present problem, the ability to simulate the spray dynamics and the validity of the radiative transfer submodel are of particular importance. The FDS code (versions 5.5.0 and 6) assessment is performed by validation and verification in the downward configuration and only by verification in the upward direction. All verifications involve comparison with the CFD code BERGAMOTE developed at the French laboratory LEMTA (Collin 2010, Lechêne 2011). This code is particularly interesting for that comparison since it differs with the FDS code. It is based on a two-way Eulerian-Lagrangian description of the dynamics of the spray (using a RANS model with a standard k-ε formulation for the turbulence modelling), combined with a Monte Carlo modelling of the radiation-spray interactions. The radiative properties are evaluated based on the Mie theory involving the exact formulation of the scattering phase function without any simplification. The gas properties are given by a C-k model with a relatively fine spectral definition (based on 43 bands or 367 bands on the whole IR spectrum).

In the downward configuration, measured and predicted attenuations have the same evolution: attenuation increases almost linearly with distance from the injection point (see Figure 2-a). This evolution results from the spray dynamics. Droplets are rapidly slowed down due to the drag force, their air residence time is also longer. The order of magnitude of attenuation is similar in the experiment and the computational simulations done by the codes BERGAMOTE and FDS (version 6). The FDS code (version 5.5.0) rather underestimates the attenuation. The discrepancy with the measured values is around 31 % with the oldest version and 11 % with the latest version, while discrepancy between the codes FDS and BERGAMOTE is around 42 % with the oldest version and 7 % with the latest version. The improvement with the latest version of FDS is related to a better description of the evolution of the true size distribution through the use of the Sauter diameter.

The upward configuration is more complex since gravity plays a stronger role and the residence time of water droplets is really longer (ten times as long (Lechêne 2010)). Due to the higher water volumetric fraction, radiation attenuation is higher in the upward configuration compared to the downward one (see Figure 2). All predicted attenuations have the same evolution: they are almost constant. The order of magnitude predicted by the two codes BERGAMOTE and FDS (version 6) is the same, it is around 70 %. The latest version of the FDS code underestimates rather these values, it predicts attenuations around 50 %. The relative discrepancy with the values predicted with the BERGAMOTE code is around 31 % with the older version and 2 % with the latest version.

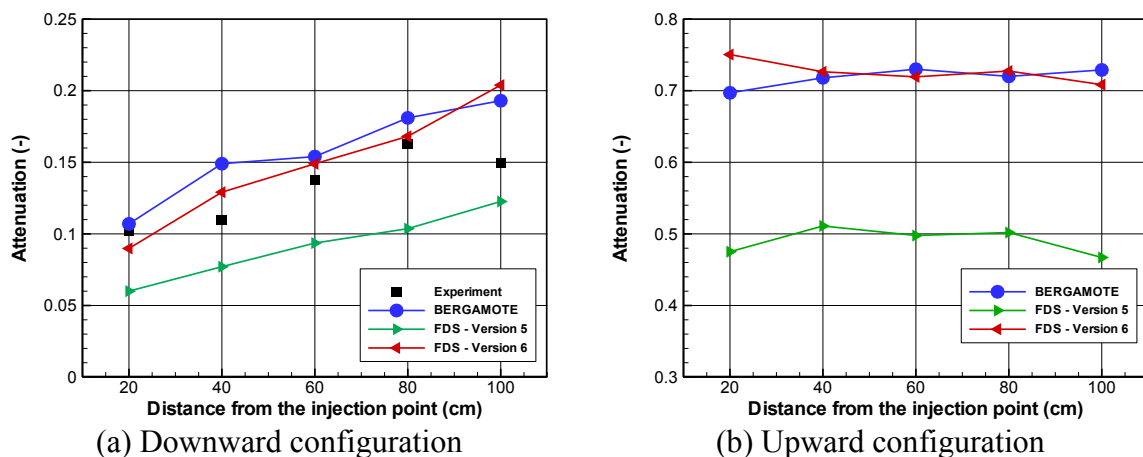


Figure 2: Radiation attenuation through the water curtain measured and predicted with the CFD codes BERGAMOTE and FDS.

Finally, based on the absolute and relative discrepancies, the FDS code (versions 5.5.0 and 6) is able to give an estimation of the radiation attenuation through the curtain along the vertical axis and this estimation appears better with the new radiative model.

Heat transfer between gas phase and droplets

For assessing the model yielding heat transfer between gaseous phase and water droplets, the approach consists in first verifying the steady state and then validating the speed at which the droplets are evaporating. The steady state is verified thanks to the first law of thermodynamics. This verification is detailed in Ref. (Blanchard 2011c), it has shown the good agreement between the thermodynamics equilibrium and the steady state predicted by the FDS code. To assess the rate of evaporation predicted, two sets of data given in Refs.

(Ranz and Marshall 1952) and (Kincaid and Longley 1989) are used. They both concern one single motionless evaporating water droplets in a given domain where air temperature is almost ambient. Since the configuration is simple and the thermal radiation could be ignored, the following work has been performed using MATLAB.

In the test conducted by Ranz and Marshall, one water droplet is placed in ambient air (24.9 °C). Its initial diameter is equal to 1048.8 μm and its temperature is 9.11 °C. The measurement deals with temporal evolution of droplet size. Figure 3-a shows a linear plot of the square droplet diameter versus time, in both experiment and simulation with the FDS model. By the way, it confirms the important cooling effect of the smallest droplets described in the Introduction. The rate of evaporation is illustrated by the curve slope on Figure 3-a. It also appears that the FDS model overestimates the rate of evaporation over the total test duration (≈11 min). The relative discrepancy between measured and predicted slopes is equal to 22.7 %. This discrepancy guarantees a good agreement during the first hundred seconds. For instance, at 90 s, the measured diameter is around 975 μm and the predicted one is equal to 967 μm. Then, this overestimation is much obvious. In particular, at 590 s, the predicted diameter is around 216 μm whereas the measured one is equal to 508 μm.

In the tests conducted by Kincaid & Longley, many parameters are tested (see (Kincaid and Longley 1989)). The only cases detailed here correspond to a relative humidity of 31 %. One water droplet is placed between 30 and 60 s in an ambient air (12.0 °C). Its initial diameter is comprised between 400 and 1500 μm and its temperature is equal to 22.0 °C. Figure 3-b shows the good agreement between measured and predicted values, discrepancy is equal to 11 %. Moreover, except for the smallest droplet, the FDS code tends to underestimate the water droplet evaporation. This trend is going against the previous trend observed in the Ranz & Marshall configuration. It also highlights the difficulty to assess this model via validations.

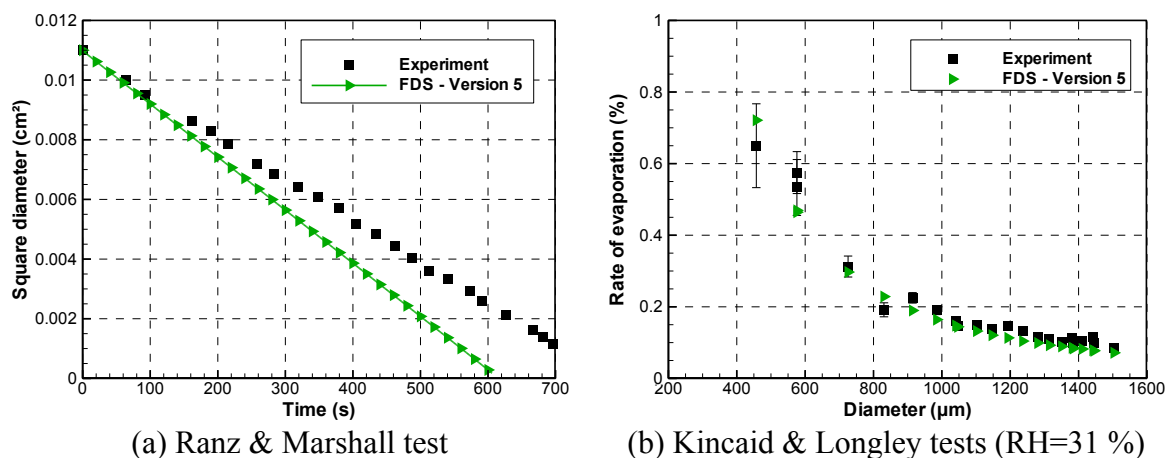


Figure 3: Rate of evaporation of water droplets measured and predicted with the FDS code

Finally, based on these 23 tests, it appears the FDS model (in version 5) is able to well predict heat transfer between gaseous phase and water droplets, especially during a short duration.

TUNNEL SCALE

After first validations using small scale tests, we now consider a larger scale configuration concerning fires in tunnel and interactions with water mist.

Test set-up

The mid-scale tunnel is 43 m long with a semi-circular cross-section around 4 m² and a 2.2 m hydraulic diameter (see Figure 4). Walls are covered by fire resistant mortar cement whose thermal characteristics are known. The floor is made of concrete.

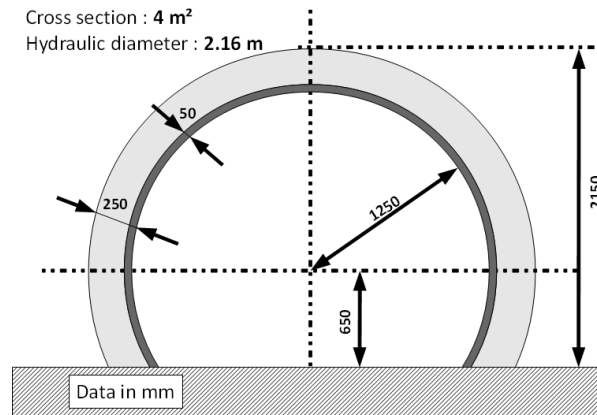


Figure 4: Cross-sectional view of the tunnel (data in mm).

188 sensors are set up in the test tunnel. They are located on four sections upstream, seven sections downstream and one at the fire location (see Figure 5). The use of so many sensors allows characterizing the environment on several whole tunnel sections. The measurements include air temperature and velocity, fuel mass, heat flux and air composition (CO₂ and O₂ concentration).

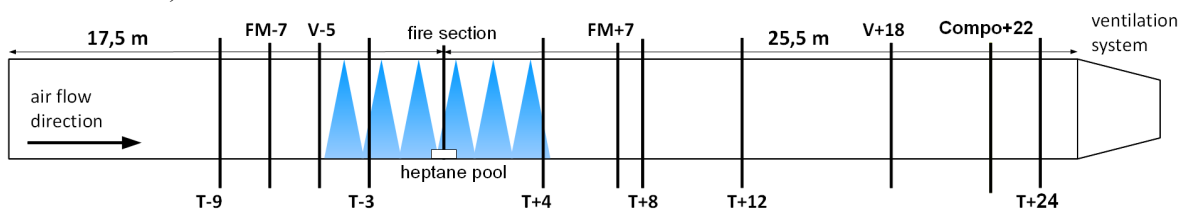


Figure 5: Position of measurement sections (*T*: temperature, *V*: air velocity, *FM*: heat flux and *Compo*: air composition). Nozzle locations are represented by blue sprays. Numbers are distances in m.

A ventilation system is mounted at the downstream side of the tunnel. It allows controlling the longitudinal air flow, by extracting a roughly constant gas volume flux. The purpose of the experimental campaign was to study two ventilation regimes, one below and one above the critical backlayering velocity (i.e. the longitudinal velocity above which all the combustion gases are transported downstream the fire). Considering the predicted fire heat release and the tunnel dimensions, the critical value has been estimated between 1.2 and 1.8 m/s, depending on the correlation used to estimate it (Blanchard 2011b). The test discussed in the present paper has been performed with an exhaust volume flux corresponding to a longitudinal velocity around 3.0 m/s. Consequently, this value induces an over-critical ventilation regime without smoke backlayering upstream the fire.

The test is conducted with a fire load produced by a 1 m×0.5 m×0.1 m heptane pool. Liquid fuel has been chosen in order to ensure repeatability between experiments and to reduce uncertainties related to the estimation of the heat release rate (HRR). The HRR is deduced from fuel weight loss monitoring and by oxygen consumption monitoring (Babrauskas 1992).

As shown in Figure 6, the HRRs deduced with the two methods are almost the same before water mist system activation. After that, deduced HRRs are clearly different. This may be due to the water spray above the fire that disturbs the heptane pool weight monitoring. The test duration corresponds to the complete burning of initial heptane quantity.

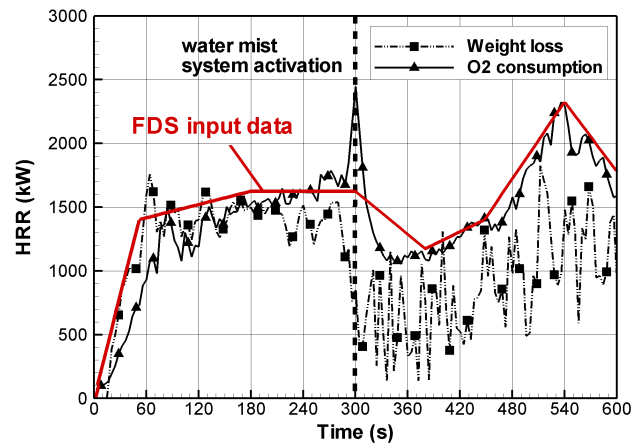


Figure 6: HRR deduced from fuel weight loss and oxygen consumption. The piecewise function used as input in the simulation is also presented.

This test is selected for the present study because of the very low injected water flow rate (as described in the next paragraph). Such academic configuration was considered instead of a huge flowrate inducing a rapid extinction, because it allows an observation of the interactions between water, fire and smoke. The main consequence is that HRR reaches a higher value during the mitigation period (300-600 s) than at the activation time 300 s. It also allows well studying the fire environment when the mitigation system is activated. For information, during the test campaign in the midscale tunnel, one test was performed in similar conditions than the present test but with a higher number of nozzles (14 nozzles). Fire was also suppressed in less than 1 min which does not allow studying surrounding conditions during mitigation.

The water mist system is composed of six nozzles located on the same row on the centre line of the tunnel. Nozzles are located between 4 m upstream and 3.5 m downstream the fire location, 1.5 m apart one other (see Figure 5). The operating pressure is around 90 bars. The water flow rate injected at each nozzle is close to 5.5 L/min, corresponding to a total mist discharge rate around 33 L/min. All the nozzles are manually activated at the same time, 300 s after ignition.

Computational input data

The mid-scale tunnel test has been simulated with the FDS code version 5.4.0. The computational domain includes the tunnel, the ventilation system at the downstream side (by setting an exhaust volume flow), and a free area at the upstream side. The last area is modelled in order to better promote the flow turbulence within the tunnel. Cubic grid cells of 10 cm are used to discretize space and the unit sphere is divided into 500 solid angles in order to solve the radiative transfer equation.

The main input data for the numerical simulation are the HRR curve, the extraction volumetric flow rate and the global combustion reaction. A HRR sensitivity analysis has been performed in order to calibrate a smoothing function from experimental heptane pool weight

loss and oxygen consumption monitoring. After water mist activation, HRR is deduced only from experimental oxygen consumption because fuel weighing is altered by droplets accumulated in the pool. The effect of water mist application on the heptane burning rate is represented by the experimental HRR curve. For this reason, FDS fire suppression model is not activated. HRR defined as input is plotted on Figure 6. The extracted gas volume flux at the downstream side is set to get a longitudinal velocity without fire around 3.0 m/s. Parameters defining the heptane combustion reaction (such as soot and carbon monoxide yields) are extracted from (Tewarson 2002).

Each nozzle installed in the midscale tunnel consists of four side injectors and one central injector. Each solid spray pattern is conic and the ejection angle has been evaluated as 20°. The orifice diameter of all injectors being around 0.5 mm, an initial velocity of 60 m/s is assumed. To calibrate the Lagrangian particle sub-models, the PDA analysis has been simulated with the FDS code, by varying mean diameter at the injection point from 20 to 60 µm. The best agreement appears to be obtained with the spray defined at the injection point with a hybrid law defined by a mean diameter and a Rosin-Rammler dispersion parameter equal to 40 µm and 2.85 respectively (see Blanchard 2011).

Validation of the FDS code

This stage consists in evaluating the discrepancy between predicted and measured quantities based upon air temperature and heat flux.

–Air Temperature–

The comparison of temperature evolutions in Figure 7 illustrates that the model predicts the thermal conditions well. Before the mitigation system activation, the comparison of predicted temperatures to measurements shows a good general agreement at most of the locations: the slope and the magnitudes are similar. More precisely, farther the measurement section from the fire is, better the numerical accuracy is. In fact, temperature tends to be under-predicted in the flame region. The bigger discrepancy is measured at mid-height in the mixing zone between the hot smoke layer in the upper part and the fresh air in the lower part. This area is better predicted by reducing the grid cell size but the corresponding computational time is very long. The numerical data being considered as sufficiently close to measurements, the refined grid is not used in the present study.

After the water mist system is activated, the gaseous phase is cooled. Air temperatures go down and become more uniform over the measurement section. The homogeneity in the air temperature over each measurement section highlights a thermal destratification. At all locations, the temperature decreases and its evolution after water mist activation is closely reproduced in the simulation, even when HRR increases again, at time around 540 s. By the end of the simulation, predicted and measured conditions correlate quite well. Whereas HRR changes, air temperatures hardly vary. However, in both simulation and experiment, a vertical thermal gradient seems to appear over each measurement section. Temperatures seem higher in the upper part of the tunnel and lower close to the floor.

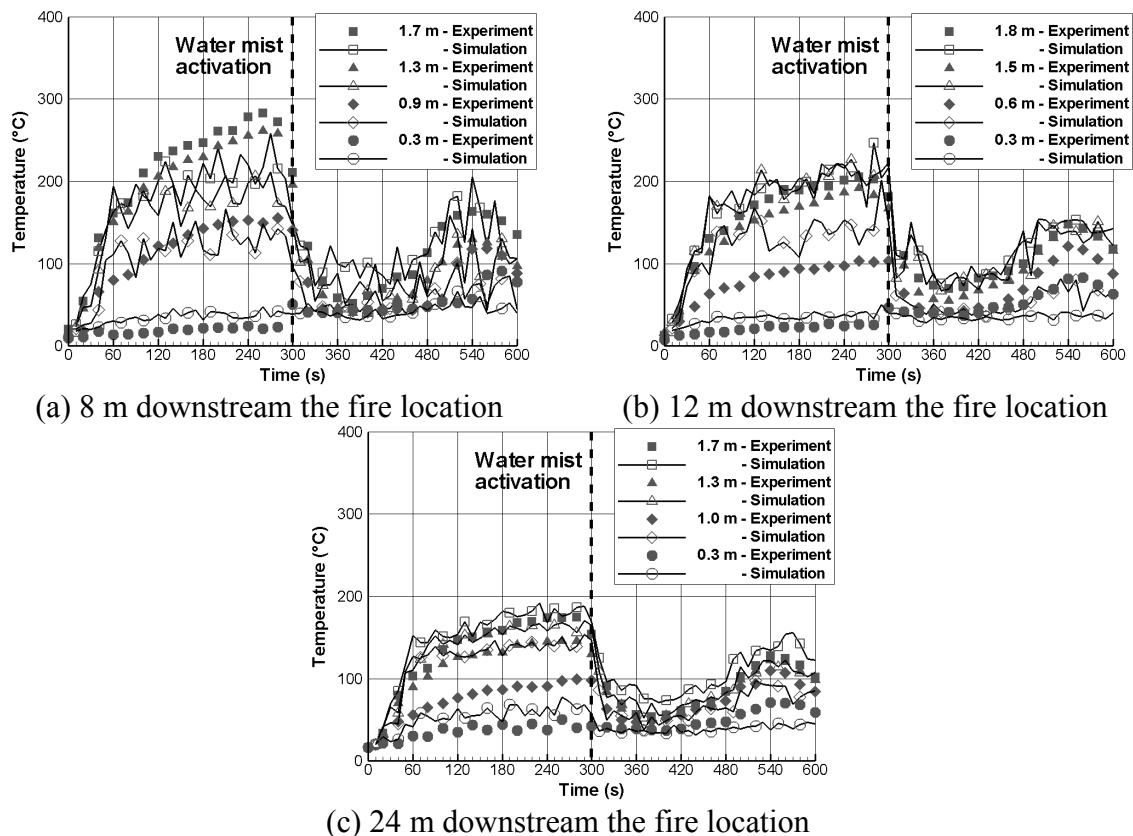


Figure 7: Simulated and measured temperatures versus time on the vertical centerline of three measurement sections (symbols for experimental data and solid line for simulation).

–Heat fluxes–

The heat flux measurements are compared with calculations on Figure 8 at different vertical positions, 7 m upstream and 7 m downstream the fire.

Upstream the fire, heat flux are very well captured by the CFD code before and after the water mist system activation. The absolute difference is below 0.17 kW/m^2 .

Downstream the fire, a heat flux is overpredicted by the code. Higher the radiometer is located, bigger the discrepancy is. This could be attributed first to the poor quality of heat flux measurement in hot smoke which is partly constituted of water vapour and soot and can also alter the measurement and secondly. After the water mist activation, it could be attributed to the water mist which likely deposits on the radiometer and could skew the measurement.

Moreover, these figures show that predicted heat fluxes are more fluctuating during the test duration compared to measurements. This difference may be attributed to measurement acquisition (every 20 s) that inevitably filters out the signal.

Interactions between water mist, tunnel longitudinal ventilation and fire

Water mist may interact with tunnel longitudinal ventilation and fire. It may also modify the tunnel air flow (mass and volumetric flow rates along the tunnel), its thermal stratification (hot layer in the upper part and colder layer in the lower part) and its toxic cartography. Moreover, water mist is affected: it is evaporated and also absorbs energy from the fire surroundings (gaseous phase, tunnel walls). Water mist is transported too. Here are only detailed the water transportation and the mist thermal contribution (see (Blanchard 2011c) for a detailed analysis).

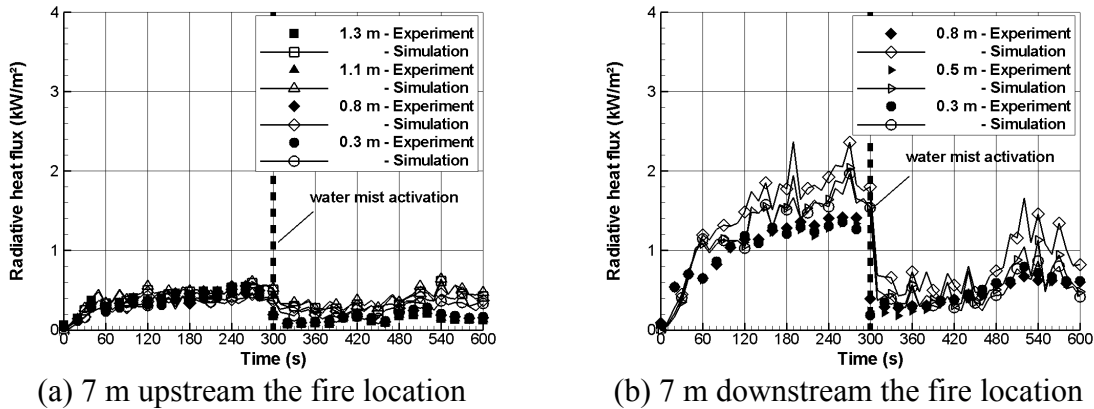


Figure 8: Simulated and measured heat flux versus time on the vertical centerline of two measurement sections (symbols for experimental data and solid line for simulation).

Figure 9 presents contours of liquid water concentration on mid-plane 540 s after ignition, i.e. 240 s after water mist system activation. This figure illustrates the water mist transportation. Whereas the activated nozzles operate from 4 m upstream to 3.5 m downstream the fire location, water droplets are transported up to 16 m downstream. The two-phase flow containing water vapor and smoke also acts as a radiative shield. It explains the low heat flux value measured and predicted downstream the fire after the water mist activation when HRR is high (see Figure 8).

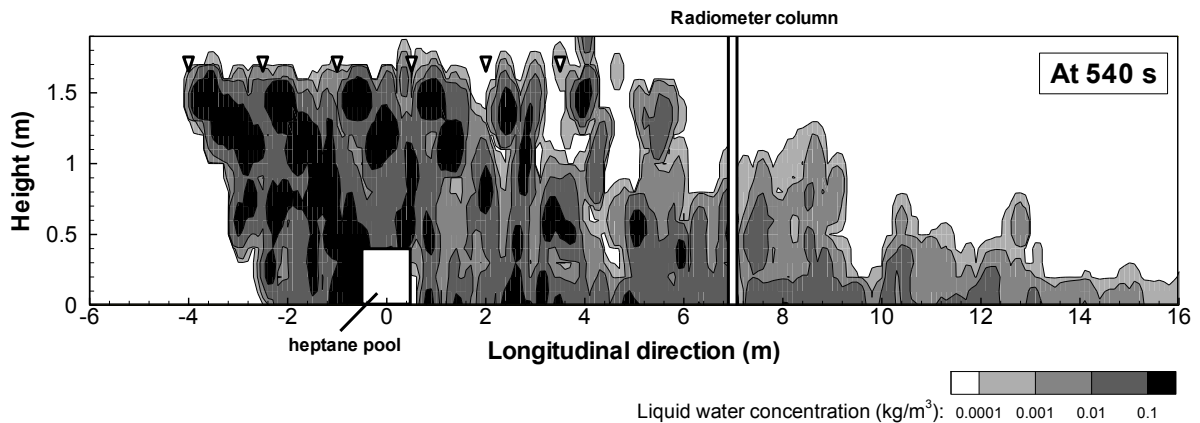


Figure 9: Contours of liquid water concentration on mid-plane in the tunnel after 540 s.

Figure 10 presents contours of temperature on mid-plane 540 s after ignition.

Our previous observation is confirmed: by the end of the simulation, HRR is high despite the water injection and the environment tends to be thermally stratified. There is an obvious thermal gradient along the vertical axis, as shown by the vertical profiles on Figure 11. Closer the measurement section from the fire is, clearer the vertical gradient is. It means that the hot gas in the upper part tends to get colder (upon contact with tunnel walls and due to the mist thermal contribution) and to mix with the fresher air in the lower part as it is flowing in the downstream direction.

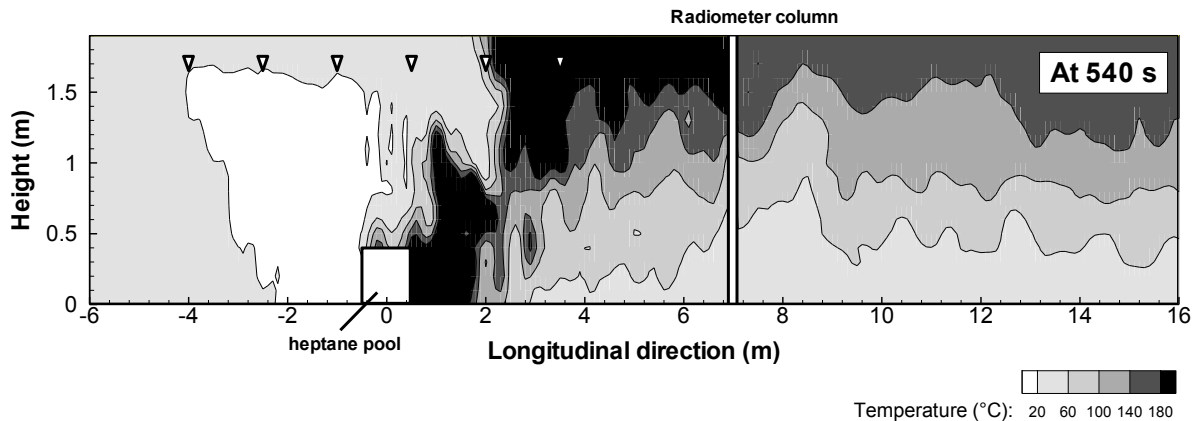


Figure 10: Temperature contours on mid-plane after 540 s.

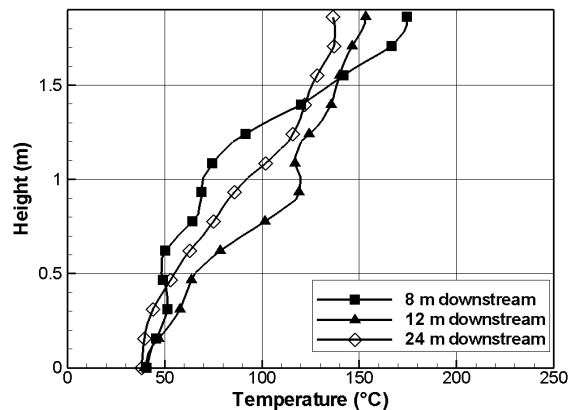


Figure 11: Vertical temperature profiles after 540 s.

The heat contribution of water mist can be estimated by performing a global energy balance with and without water mist for the whole tunnel (Blanchard 2011). The method consists in extracting and collecting information from FDS calculation by adding a subroutine in the dump file. This subroutine does not modify the physical sub-models, it allows to extract additional outputs that are not a part of the official FDS version. Conservation of energy holds that the fire heat release Q_{fire} :

- goes to heat the gases within the domain, noted Q_g ,
- is transferred to wall boundaries by radiation and convection, noted Q_w ,
- is transported through the openings, noted Q_d ,
- is absorbed by the droplets Q_p .

Figure 12 illustrates this global energy balance as a function of time. Before water mist system activation, the energy balance highlights that nearly the half quantity of fire heat is lost toward tunnel walls. The remaining heat goes into gases through the openings and for heating. After water mist system activation, water droplets are introduced into the fire environment inducing gas and surface cooling and radiation attenuation. Figure 12 shows that water mist has a strong influence. The energy balance yields that roughly the half quantity of fire heat is absorbed by droplets. The remaining quantity goes to heat tunnel surface (24 %) or is conveyed by hot gases out of the tunnel (33 %).

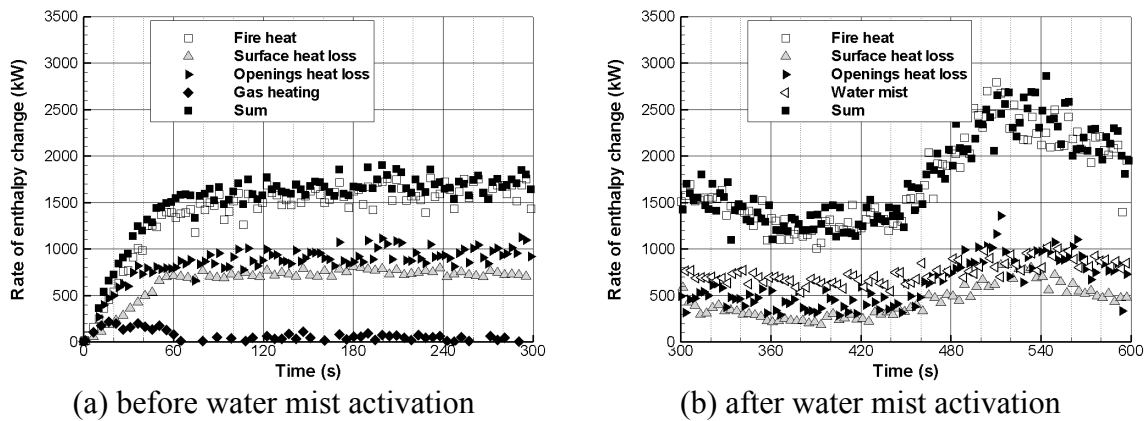


Figure 12: Energy balance applied to test tunnel.

Droplet contribution can be analyzed more in details. This study is reported in Figure 13. The distribution is almost constant between 300 and 600 s. The energy absorbed by droplets mainly comes from gaseous phase (73 %). In other words, 73 % of absorbed energy due to droplets induces a gaseous phase cooling. The last 27 % of fire heat absorbed by droplets results from radiative attenuation (18 %) and wall surface cooling (9 %).

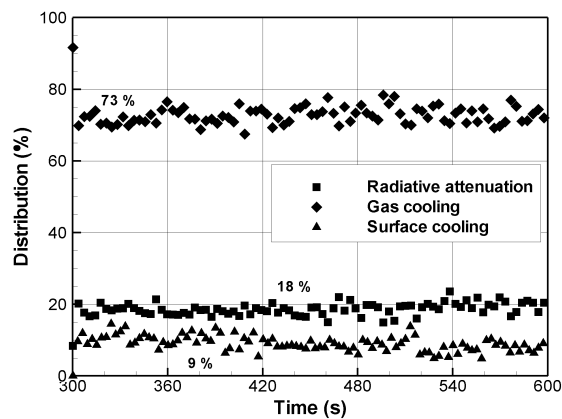


Figure 13: The rate of absorbed heat by water droplets versus time (radiative attenuation ■, gas cooling ◆, and surface cooling ▲).

CONCLUSIONS

A series of experimentations and numerical simulations has been reported from laboratory scale up to large scale on fire and fire suppression by water mist. The global context aims at validating some of the relevant sub-models when using laboratory scale tests, or testing a complete numerical code – FDS in the present study – when dealing with a real fire.

The radiative transfer model and the evaporation submodel have been tested in particular, showing a good ability to deal with these complex parts of the fire simulation when using FDS. Regarding a complete simulation of a fire in a tunnel, the prediction shows a satisfactory agreement when considering temperature, velocity or heat flux distributions.

Beside this validation step, the numerical simulation provides a tool for better understanding the action of water mist on the fire. Water mist may interact with tunnel longitudinal ventilation, smoke and fire activity. It also modifies the tunnel air flow (mass and volumetric flow rates along the tunnel), its thermal stratification (hot layer in the upper part and colder layer in the lower part) and its toxic cartography. For instance, droplets introduced in fire

surroundings absorb the half fire heat. Moreover, through a dedicated energy balance performed on the tunnel, water droplets have been observed to mainly cool the gases in the tunnel, due to evaporation phenomena. The other actions of water are radiation shielding and wall heat exchange. These trends were expected, but the numerical tool provides a quantification of the respective effects. Moreover, it could further be used to estimate the alteration of these physical phenomena when varying the water flow rate or the droplet size distribution for example.

REFERENCES

- NFPA 750: Standard on Water Mist Fire Protection Systems, 2010 Edition.
- Bergqvist, A., Frantzich, H., Hasselrot, K. and Ingason, H. (2005) “*Fire and rescue operations in tunnel fires: a discussion of some practical issues*” in *The Handbook of Tunnel Fire Safety*, Thomas Telford Publishing, ISBN 978-072-773-168-5.
- Babrauskas, V., Grayson, S.J., Janssens, M. and Parker, W.J. (1992) “*Heat Release in Fires*”, Elsevier science publishers, ISBN 978-095-565-484-8.
- Blanchard, E., Desanghere, S. and Boulet, P. (2011) “*Quantification of energy balance during fire suppression by water mist in a mid-scale test tunnel*”, *Fire Safety Science* 10.
- Blanchard, E., Boulet, P., Desanghere, S., Cesmat, E. Meyrand, R., Garo, J.P. and Vantelon, J.P. (2011b) “*Experimental and numerical study of fire in a midscale test tunnel*”, *Fire Safety Journal*, DOI number 10.1016/j.firesaf.2011.09.009.
- Blanchard, E. (2011c) “*Modélisation de l’interaction entre un brouillard d’eau et un feu en tunnel*”, PhD Thesis, Université Henri Poincaré – Nancy 1, pp. 1-236.
- Cochard, S. (2003) “*Validation of Fire Dynamics Simulator (version 2.0) freeware*”, *Tunnel Management International Journal*, Volume 6, pp. 32-37.
- Collin, A., Lechene, S., Boulet, P. and Parent, G. (2010) “*Water mist and radiation interactions: application to a water curtain used as a radiative shield*”, *Numerical Heat Transfer, Part A: Applications*, Volume 57, pp.537-553.
- Dubay, C. and Mawhinney, J. R. (1999) “*Water Mist Technology Evolves*”, *NFPA Journal* 93, Volume 6, pp. 58-65.
- Grant, G., Brenton, J. and Drysdale, D. (2000) “*Fire suppression by water sprays*”, *Progress in Energy and Combustion Science*, Volume 26, pp. 79-130.
- Heskestad, G. (2002) “*Scaling the interaction of water sprays and flames*”, *Fire Safety Journal*, Volume 37, pp. 535-48.
- Husted, B.P. (2007) “*Experimental measurements of water mist systems and implication for modelling in CFD*”, PhD Thesis, Lund University, pp. 133.
- Ingason, H. and Lönnemark, A. (2005) “*Heat release rates from heavy goods vehicle trailer fires in tunnels*”, *Fire Safety Journal*, Volume 40, pp. 646-668.
- Kincaid, D. C. and Longley, T. S. (1989) “*A water droplet evaporation and temperature model*”, *Transactions of the American Society of Agricultural Engineers (ASAE)*, Volume 32, pp. 457-463.
- Lechêne, S. (2010) “*Etude expérimentale et numérique des rideaux d’eau pour la protection contre le rayonnement thermique*”, PhD Thesis (available in French), Université Henri Poincaré – Nancy Université, pp. 217.
- Lechêne S., Acem Z., Parent G., Jeandel G. and Boulet P. (2011) “*Upward vs downward injection of droplets for the optimization of a radiative shield*”, *Int. J. Heat Mass Transfer*, Volume 54 (9-10), pp. 1689-1697.
- Mawhinney, J. R. (2011) “*Fixed fire protection systems in tunnels: Issues and directions*”, *Fire Technology*, Volume 47, pp. 1-32.

- McGrattan, K. and Hamins, A. (2001) “*Numerical simulation of the Howard Street tunnel fire, Baltimore, Maryland, July 2001*”, National Institute of Standards and Technology Report NISTIR 6902, Gaithersburg, MD, pp. 41.
- McGrattan, K., McDermott, R., Hostikka, S. and Floyd, J. (2010) “*Fire Dynamics Simulator (Version 5), User's Guide*”, National Institute of Standards and Technology Special Publication 1019-5, Gaithersburg, MD, pp. 246.
- McGrattan, K., Hostikka, S., Floyd, J., Baum, H., Rehm, R., Mell, R. and McDermott, R. (2010) “*Fire Dynamics Simulator (Version 5), Technical Reference Guide, Volume 1: Mathematical Model*”, National Institute of Standards and Technology Special Publication 1018-5, Gaithersburg, MD, pp. 124.
- Modest, M. F. (2003) “*Radiative heat transfer*” (2nd Edition) Elsevier Academic Press, ISBN 978-012-503-163-9.
- Ranz, W. E. and Marshall (1952) “*Evaporation from drops - part II*” Chemical Engineering Progress, Volume 48, pp. 173-180.
- Tewarson, A. (2002) “*Generation of heat and chemical compounds in fires*” in The SFPE Handbook of Fire Protection Engineering (3rd edition), National Fire Protection Association, Quincy, MA 02269, 2002.
- Yoshida, A., Uendo, T., Takasaki, R., Naito, H. and Saso, Y. (2011) “*Water droplets behavior in extinguishing methane-air counterflow diffusion flames*”, Fire Safety Science 10.

